RESPONSIVE CITIES SYMPOSIUM

COLLECTIVE INTELLIGENCE DESIGN

BARCELONA
27.11 – 28.11

SYMPOSIUM PROCEEDINGS

2023

RESPONSIVE CITIES SYMPOSIUM

COLLECTIVE
INTELLIGENCE DESIGN

SYMPOSIUM

PROCEEDINGS

2023

RESPONSIVE CITIES
COLLECTIVE INTELLIGENCE DESIGN

RESPONSIVE CITIES: COLLECTIVE INTELLIGENCE DESIGN
SYMPOSIUM PROCEEDINGS 2023

Disseny Hub Barcelona
C. Irena Sendler, 1, 08018, Barcelona
27-28 November 2023

ISBN-978-84-120885-7-1

EDITORS:
Areti Markopoulou
Chiara Farinea
Mathilde Marengo

LAYOUT:
Aleyna Gültekin

COORDINATION:
Fiona Demeur

PUBLISHED BY:
Institut d'Arquitectura Avançada de Catalunya
Pujades 102 baixos, Poble Nou
08005 Barcelona, ES
www.iaac.net

ORGANIZED BY:

PARTNERS OF THE PROJECT:

WITH THE SUPPORT OF:

Co-funded by the European Union

INSTITUTE FOR ADVANCED
ARCHITECTURE OF CATALONIA

ADVANCED ARCHITECTURE GROUP

QRES

A QGIS plugin to calculate resilience based on the proximity of urban resources

LUIGI PINTACUDA
University of Hertfordshire, UK
l.pintacuda@herts.ac.uk

SILVIO CARTA
University of Greenwich, UK
silvio.carta@gre.ac.uk

TOMMASO TURCHI
University of Pisa, Italy
tommaso.turchi@unipi.it

MAURO SABIU
MKS D-Tech Ltd, UK
mauro@mksdtech.com

KEYWORDS
QGIS, Resilient Communities, Isochrones, Urban Analysis, Urban Predictions, Simulations

ABSTRACT
This study presents our latest development of a plugin for QGIS to help designers and planners to calculate resilience values for specific areas in urban contexts. Instead of radial distance, the proposed approach considers isochrones as the main driver of the computation, considering the time required to reach each urban typology, thus accounting for the constraints of specific environments and providing more accurate results. This study illustrates how more accurate methods of time calculation in the built environment can address climate adaptation and urban performance of communities with promising results.

1. INTRODUCTION

The present study builds on previous work our team carried out on resilient urban communities and the measurement of their characteristics through quantitative methods. With this study, we address the symposium theme of "Adapt to Climate & Perform", synthetic ecologies, simulating, and predicting by presenting a novel workflow based the on prediction of resilience values estimated directly on screen.

The design of the physical environment is a key element in the complex web of variables that affect how people interact with and use urban places. The layout of the physical environment greatly influences how people interact with and move through metropolitan areas. The availability, placement, and organization of resources within neighborhoods and cities play a crucial role in determining how urban communities react to certain occurrences. Communities survive, adapt, and thrive within and around the physical components of their urban environs, whether confronted with more gradual changes like those caused by climate change or unexpected tragedies like earthquakes or flooding.

2. EXISTING WORK AND BACKGROUND

There are a growing number of studies focusing on urban analytics and simulation for urban resilience. The following section includes a summary of some of the most recent tools addressing elements of urban resilience.

2.1 EXISTING WORK

In urban resilience studies, there is a growing body of literature that considers principles, indicators, criteria, and conceptual frameworks for resilience (e.g., Quinlan et al. 2016) and its calculation in both qualitative and quantitative terms (Tyler and Moench 2012; Jha et al. 2013; Silva and Morera 2014; Sharifi and Yamagata 2016, among many others). However, the study and development of operational tools are less prominent, as they tend to focus on specific actions and objectives, rather than the broader socio-economic factors found in general resilience work.

Wardekker et al. (2020) proposed a tool that works with a three-step approach: preparation and goal setting, diagnosis of selected aspects (of resilience), and a reflective step where the consequences of the choices made during the process are considered (Wardekker et al. 2020:6-7). This tool is diagnostic and analytic, and it can be quite effective in identifying key factors at play in measuring and predicting resilience from literature and policy documents. Similarly, Khazai et al. (2018) developed an approach to resilience measurement based on key dimensions that include social capacity, legal and institutional arrangements, emergency preparedness and response and recovery among others (Khazai et al. 2018). They developed a Resilience Performance Scorecard structured in three consecutive stages: development of resilience dimensions, facilitating the participatory approach, and self-assessment. This tool is quite useful in participatory approaches in specific locations, yet it does not address the peculiarities of the built urban environment as primary objectives.

Dianat et al. (2022) produced a robust method to assess urban resilience tools. They considered frameworks like the City Resilience Index (ARUP and Rockefeller Foundation 2014) and the Grosvenor Resilient Cities Index (Grosvenor 2014). This method is useful to assess frameworks and general resilience tools, but it does not consider computational tools.

There are a number of other operational tools that support the measurement of urban resilience through computational methods. URBANO (Dogan et al. 2020) is a suite of methods that help designers to measure urban features including people's amenity demand, the use of a given street per trips, and the walkability rating. This tool focuses on mobility modelling and urban amenity analysis but can also contribute to urban resilience calculation. Similarly, tools like the Spatial Design Network Analysis (Cooper and Chiaradia 2020) allow for a space-syntax based spatial network analytics that can be used to retrieve values to be used in a resilience model. While such tools and methods are powerful in providing urban data, our tool specifically targets urban resilience, using a mathematical model we developed in previous work (see Carta et al. 2021).

2.2 MEASURING RESILIENCE: METHODOLOGY

Our work examines how the availability, placement, and arrangement of resources within urban areas influence the way in which communities react to different events: from immediate disasters to gradual environmental changes. The study is underpinned by the idea that there is a strong relationship between urban morphology and community resilience. In this context, we explore the significance of connectedness within urban structures and its function in both desirable and undesired occurrences, commenting on the crucial value of measuring and forecasting resilience for efficient urban design. In previous work (Carta et al. 2021), we modelled community resilience as:

$$R = \sum_{i=1}^{n} d(\,)_i \gamma_i$$

where the minimum distance d (min) from the neighborhood center to a particular urban feature (such as a school or park) is considered to determine the overall resilience value R for a neighborhood. ϒ is a coefficient that evaluates the quality of this distance based on established research and reports (Carta et al. 2021). Our research addresses the important issues surrounding the choice of suitable resilience measures, their consequences for urban design, and the comprehension of the scales related to these metrics. The resulting patterns of proximity and density, and initial linkages among urban typologies demonstrate the potential of our creative approach because they are frequently hidden in conventional maps and pre-existing resilience frameworks.

3. DEVELOPMENT OF THE QGIS PLUGIN

This study is based on the development of a QGIS plugin where distances d(min) are calculated as isochrones, instead of as Euclidean distances like in previous applications. Isochrones are defined as lines connecting points with equal travel times (see O'Sullivan et al. 2000). Results of previous stages of this study have been published in Carta et al. 2021, 2022, 2023. As in our previous study, we take into consideration the redundancy of features; this gives us back some hyper-resilient points (R-value>1). In the output stage, the plugin assigns a total resilience value and a specific value for each feature for each point, enabling quick comparisons between different areas.

3.1 PLUGIN WORKFLOW

The plugin workflow can be easily explained by looking at the three main macro-operations:

1. Extract;

2. Compute;

3. Produce the output.

In the extraction stage, for each point of a user-created layer, the plugin retrieves selected features (which, at this stage of development, are still a predefined set) and specific isochrones, with varying time sizes based on feature accessibility, using data from our previous study (Carta et al. 2021, 2023). We chose OpenStreetMap (OSM) data as it is open-source, can be integrated with QGIS, and has a global dataset. We selected MapBox (MP) for isochrone services as it is more reliable and performant than our initial choice, OpenRouteService (ORS). Despite MP being a commercial service and ORS being open-source, we opted for MP due to its quicker response time for extracting isochrones. In this study, we employed approximately 35,000 isochrones in the testing phase. However, the plugin was coded to minimize the number of isochrone requests to improve the performance. Once the isochrones were retrieved, the plugin evaluated the resilience for each point using an updated method from our previous approach (Carta et al. 2021, 2023). The isochrones could be generated based on different means of transportation, like walking, cycling, or driving, allowing for more precise control and tuning of each feature. In the output stage, the plugin assigned a total resilience value and a specific value for each feature at each point.

3.2 INITIAL TESTING

In this text, we are presenting the initial tests we ran comparing the results obtained with our QRES against our previous work (Carta et al. 2021, 2022, 2023) and other established frameworks, including the NUMBEO (2021) Quality of Life and the Grosvenor (2014) Resilient Cities Index. The primary objective of the tests is to understand how the plugin produces reliable results using different point samples to optimize the analysis for various scales and define the level of detail required. The data generated by our engine are rendered through heatmaps using the Kernel Density Estimation (KDE) method. KDE is one of the prevailing techniques for 2D spatial analysis in GIS applications (Gadzinski 2015; Nakaya and Yano 2010). KDE creates continuous density surfaces after assessing localized hotspots, allowing users to view the spatial distribution of a specific value (Thompson et al. 2011). Its accuracy depends on the density of the samples.

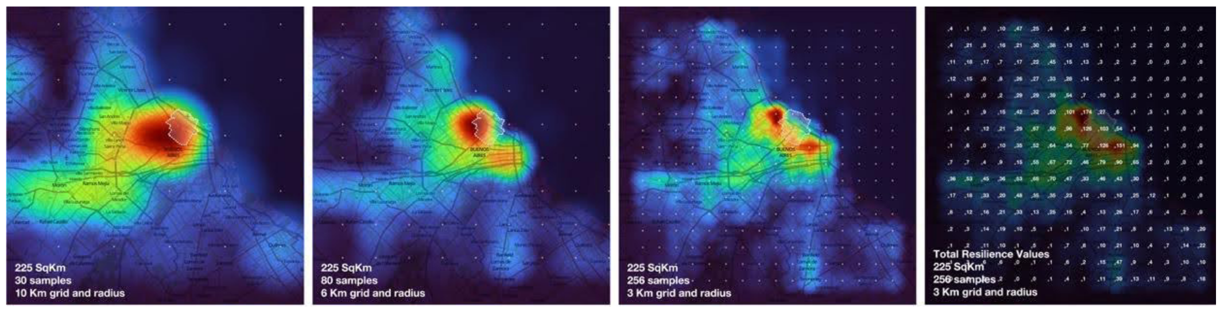

Figure 1:
Different point grids for the same area

In Figure 1, we conducted tests on a 225 km2 area in Buenos Aires, utilizing points grids with different spacings: 10, 6 and 3 km (30, 80, and 256 samples). Visual analysis indicates that finer grids result in greater accuracy, but at the expense of longer calculation times. However, even with a grid of 30 samples, we can gain insights into the city's overall resilience. In each of these examples, the heat map's radius is set to match the distance between the samples.

In Figure 2, we zoomed in on a 100 km2 area near the Palermo district, considered the most livable area based on qualitative assessment (SAVA 2018). At this scale, using samples with a 10 km distance results in a generic outcome, with a large red spot at the center. In the 6 km grid, two distinct red areas become evident. Notably, the 3 km and 1 km grids yield similar results. Based on typical walking distances, the 1 km grid appears optimal, as people can cover 1.2 to 1.6 km in a straight line.

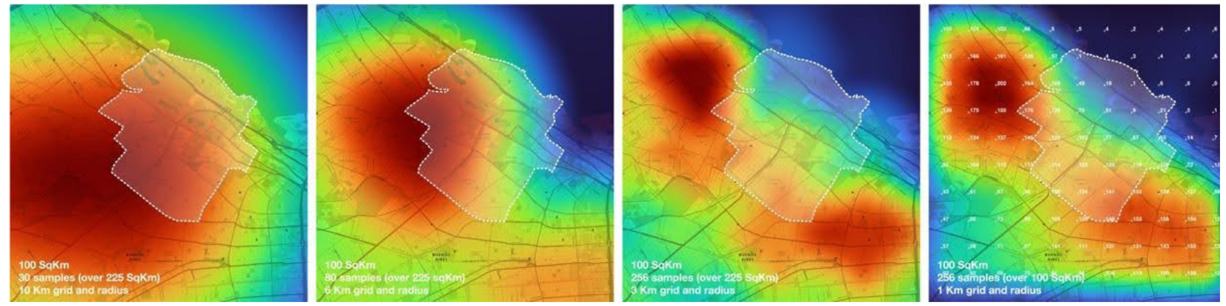

Figure 2:
Different points grids on the same area

Considering that the heat map (KDE) is significantly influenced by the density of data points, we note that a regular grid tends to yield a more efficient spatial distribution of Resilience values. In Figure 3, we conducted tests within the same 225 km2 area using an 80-point regular sample (as demonstrated in Figure 1, this exhibits high reliability) and compared this with an 80-point random distribution. Even with a broader radius, the latter approach results in inaccurate outcomes due to the uneven distribution of points.

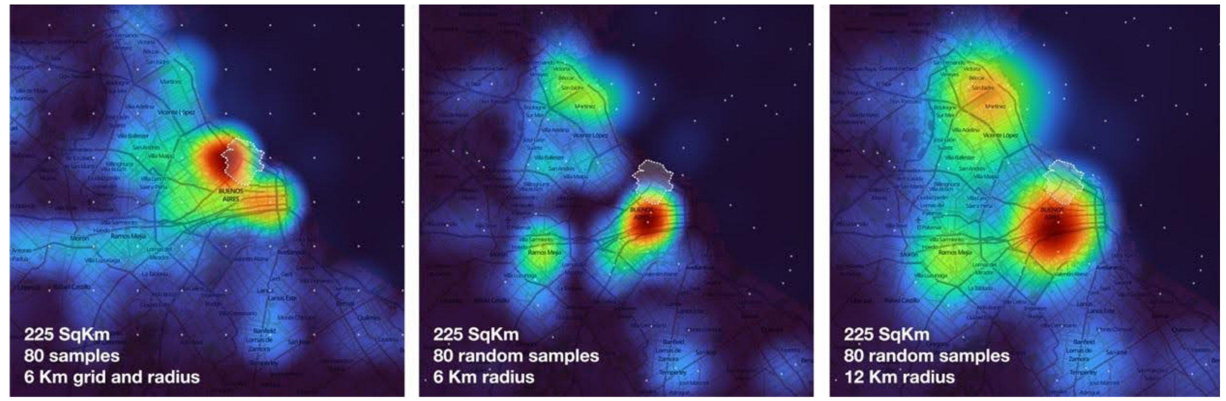

Figure 3:
Regular vs. random points grid

Given that the regular grid proves to be the more efficient approach, the most effective heat map radius corresponds to the spacing of the grid. Employing a radius smaller than this would preclude interactions between points, while a substantially larger radius would result in a loss of detail (Figure 4).

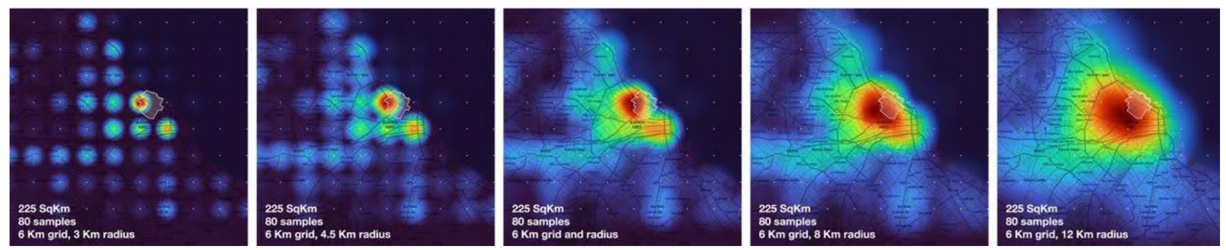

Figure 4:
Same grid and different radius values

Since the Resilience value is relative to the specific calculation and not associated with any established metric, users have the option to set their heat map preferred maximum value. Keeping it on "auto" (indicating the maximum sample R value) produces a clearer map (Figure 5). However, this value can be manually set as required. In the second map in Figure 5, the maximum value is 20 (areas with R>20 are rendered in red), and we set a color scale where R=1 is represented by the color green. In the third map, the maximum value is set to 1, designating areas R>1 in red.

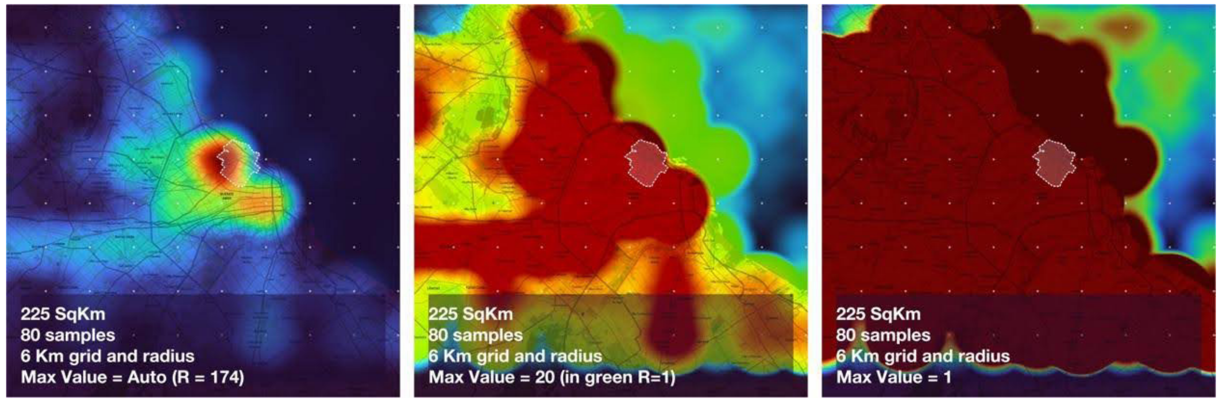

Figure 5:
Different R maximum values

The plugin offers the option to break the analysis down (Figure 6), allowing for the creation of maps for each feature. This capability holds significant importance for urban planners and designers as it helps to quickly identify areas in need of improvement for specific features. As we advance in the plugin's development, this breakdown becomes crucial for the introduction of interactive functions, empowering users to simulate the incorporation of specific facilities and assess cities' performance following their integration.

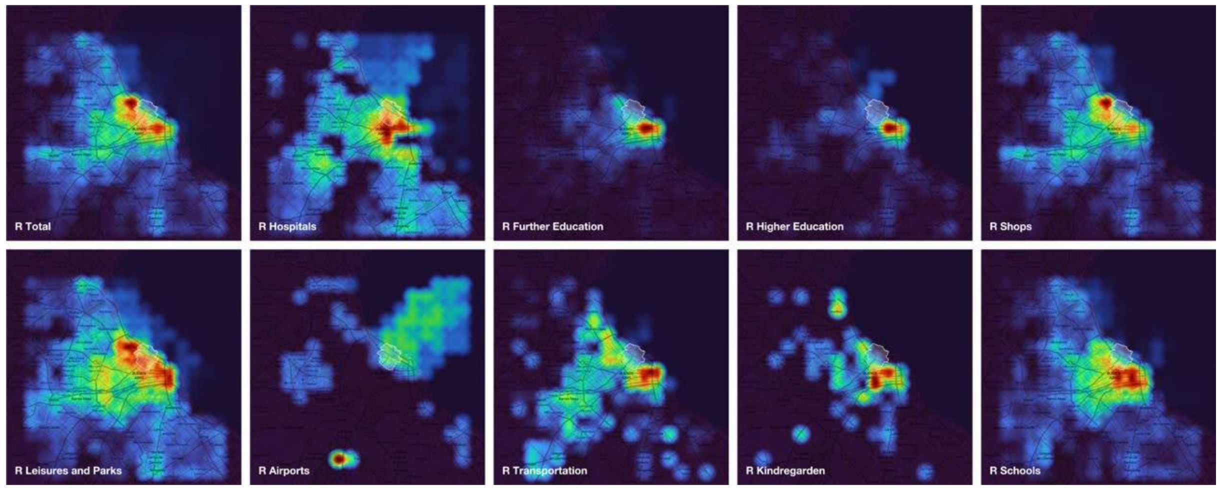

Figure 6:
Breakdown of the different features: hospitals, continuing education, higher education, shops, leisure and parks, airports, transportation, day care, schools

We generated new maps (Figure 7) for the 16 different cities in our previous work (Carta et al. 2023). These are featured in both the Grosvenor (2014) Quality of Life Global Ranking and the Quality of Life (QOL) global ranking from Numbeo (2021). This analysis builds upon the work of Tapsuwan et al. (2018), who connected the concepts of livability and QOL to sustainable living and resilience within the context of urban development. The graphic output of our QRES analysis reveals a consistent pattern across all the samples: the most livable areas (Carta et al. 2023) are situated on the fringes of the most high-performing areas in each city. This demonstrates that QOL accounts for proximity to features and the avoidance of densely

crowded areas with excessive urban features, which can lead to a chaotic and busy environment.

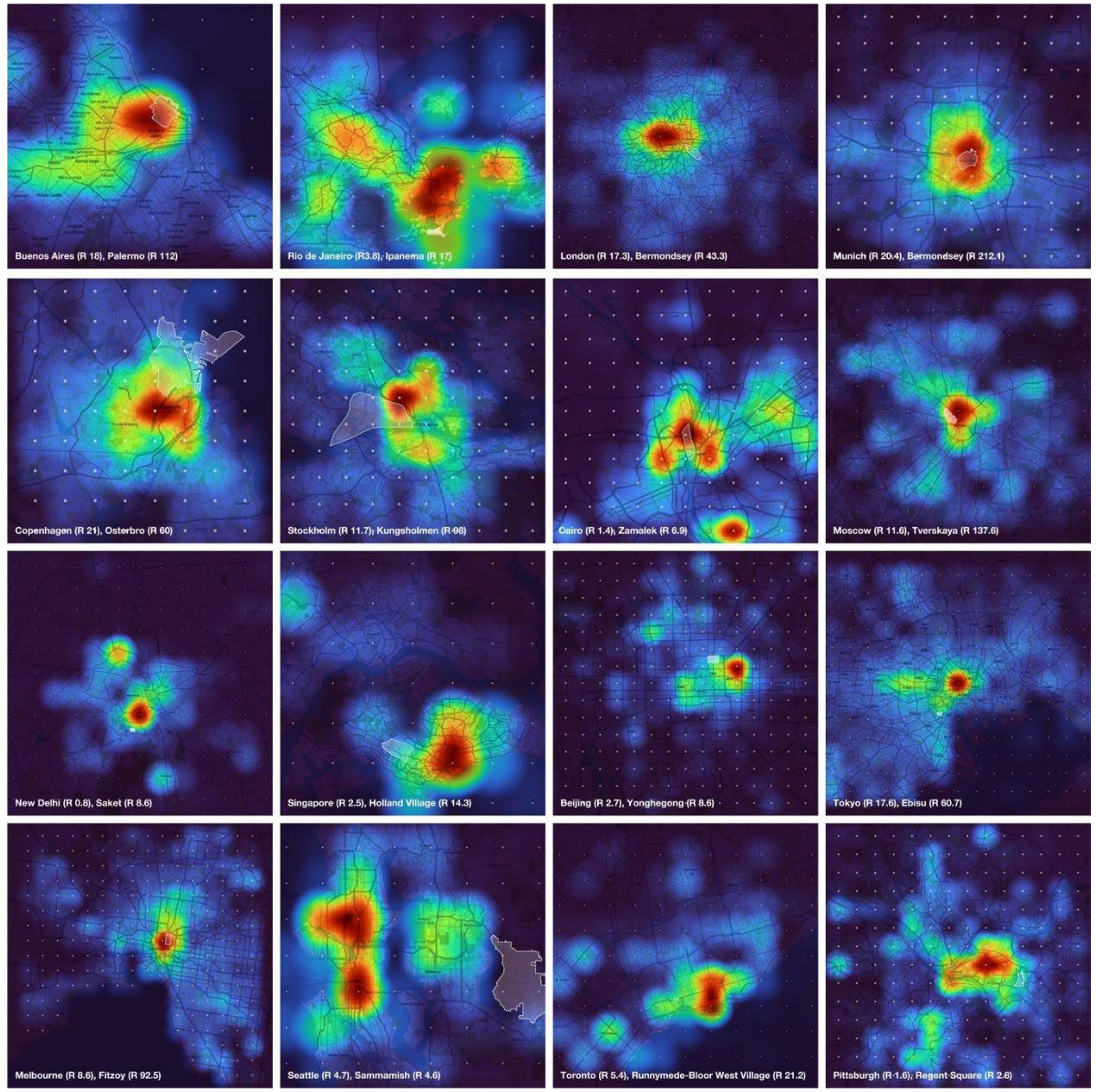

Figure 7:
Analysis of 16 different cities, most livable areas dashed in white

However, it is worth noting that the case of Seattle deviates from this pattern (Figure 8). This presented us with a valuable opportunity to leverage the plugin to re-evaluate our previous findings and delve deeper into the issue. Initially, the Sammamish area was provided to us through a qualitative assessment (Kolmar, 2022). However, this assessment focused on suburban areas: the resilience for Sammamish mirrored the Seattle overall average, rather than overperforming. In response to this, we turned to other qualitative sources (Bungalow, 2023), and we proceeded to analyze the three top areas. Interestingly, all of these areas conformed to the established pattern previously observed in other cities.

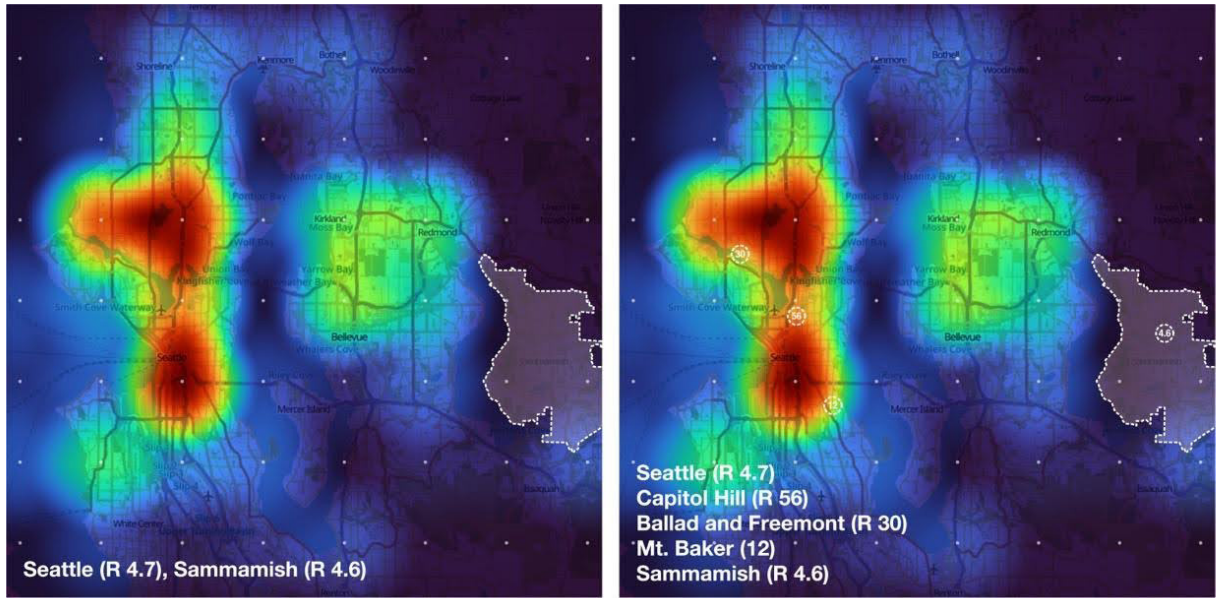

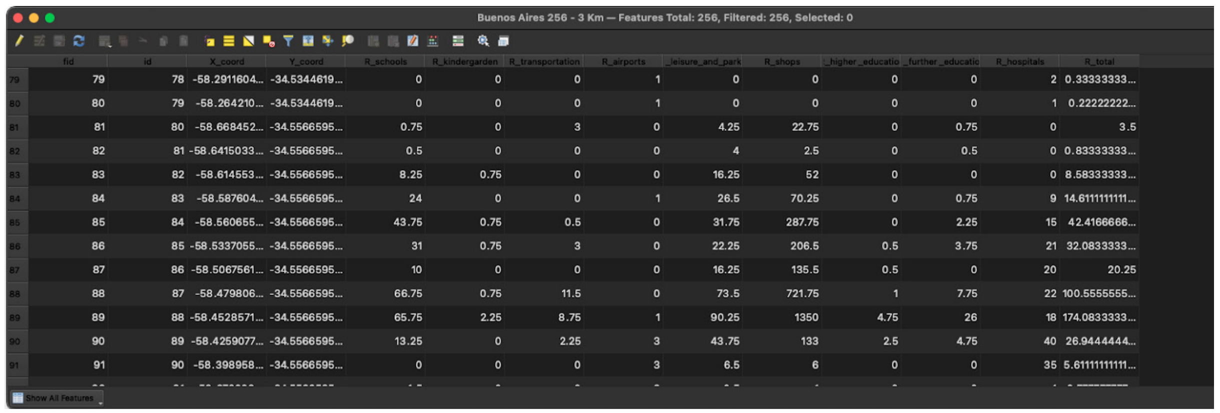

Buenos Aires 256 - 3 Km — Features Total: 256, Filtered: 256, Selected: 0

	fid	id	X_coord	Y_coord	R_schools	R_kindergarden	R_transportation	R_airports	_leisure_and_park	R_shops	_higher_educatio	_further_educatio	R_hospitals	R_total
79	79	78	-58.2911604...	-34.5344619...	0	0	0	1	0	0	0	0	2	0.33333333...
80	80	79	-58.264210...	-34.5344619...	0	0	0	1	0	0	0	0	1	0.22222222...
81	81	80	-58.668452...	-34.5566595...	0.75	0	3	0	4.25	22.75	0	0.75	0	3.5
82	82	81	-58.6415033...	-34.5566595...	0.5	0	0	0	4	2.5	0	0.5	0	0.83333333...
83	83	82	-58.614553...	-34.5566595...	8.25	0.75	0	0	16.25	52	0	0	0	8.58333333...
84	84	83	-58.587604...	-34.5566595...	24	0	0	1	26.5	70.25	0	0.75	9	14.6111111111...
85	85	84	-58.560655...	-34.5566595...	43.75	0.75	0.5	0	31.75	287.75	0	2.25	15	42.4166666...
86	86	85	-58.5337055...	-34.5566595...	31	0.75	3	0	22.25	206.5	0.5	3.75	21	32.0833333...
87	87	86	-58.5067561...	-34.5566595...	10	0	0	0	16.25	135.5	0.5	0	20	20.25
88	88	87	-58.479806...	-34.5566595...	66.75	0.75	11.5	0	73.5	721.75	1	7.75	22	100.5555555...
89	89	88	-58.4528571...	-34.5566595...	65.75	2.25	8.75	1	90.25	1350	4.75	26	18	174.0833333...
90	90	89	-58.4259077...	-34.5566595...	13.25	0	2.25	3	43.75	133	2.5	4.75	40	26.9444444...
91	91	90	-58.398958...	-34.5566595...	0	0	0	3	6.5	6	0	0	35	5.61111111111...

Show All Features

Figure 8:
Analysis of Seattle

Figure 9:
Sample of a QGIS attribute table

The plugin also generates a numerical attribute table, which can be exported as a .csv file (Figure 9) for further data utilization. This capability enabled us to conduct a comparison between this study against our prior methodologies employing Rhino + Grasshopper (GH) (Carta et al., 2021), RECOMM (Carta et al., 2023) and two well-established resilience indices, namely the QoL (Numbeo 2021), and the Grosvenor (2014) Resilient Cities Index (Table 1).

Furthermore, the .csv output enabled us to conduct several graphic comparisons. We assessed how the most livable areas fared when using our GH method as compared to QRES. Since both methods rely on the proximity of features, the trends of the two curves exhibit similarities. However, as QRES uses isochrones, it provides more accurate results.

When comparing the QRES results for entire cities with the most livable areas (Figure 10), some discrepancies arise due to the diverse nature of zones within large cities, where not all areas exhibit uniform performances. Notably, there are some inconsistencies, such as in London, where the city as a whole performs better than expected, which represents a positive aspect. However, the presence of points over bodies of water can lower the city's overall performance due to their lower R score.

CITIES	QRES R AWG	QRES R M. Liveable	R (QoL)	R (GSVN)	R (GH)	RECOMMENDED
Beijing	2.677654321	8.63888889	234	39	7.39	1.43
Buenos Aires	18.05772569	112.666667	213	26	4.06	1.12
Cairo	1.425390266	6.94444444	227	48	5.89	5.48
London	17.302469	43.3055556	236	42	4.92	0.79
Melbourne	8.5722483	92.5277778	149	18	4.82	-
Moscow	11.5810887	137.583333	44	13	6.7	1.24
Munich	20.3688889	212.166667	202	37	5.78	-
New Delhi	0.84312678	8.55555556	27	24	14.14	9.48
Pittsburgh	1.59311224	2.83333333	47	5	6.55	-
Rio de Janeiro	3.82373114	17	232	45	6.7	1.22
Seattle	7.77314815	55.94444444	26	11	7.56	3.08
Singapore	2.5334467	14.333333	113	32	4.53	-
Stockholm	11.7105556	98.0277778	92	6	3.92	1.25
Tokyo	17.5641026	60.6666667	87	26	6.97	1.47
Toronto	5.41919192	21.2777778	101	1	4.69	1.31

Table 1:
Comparison of different R values obtained with multiple methods

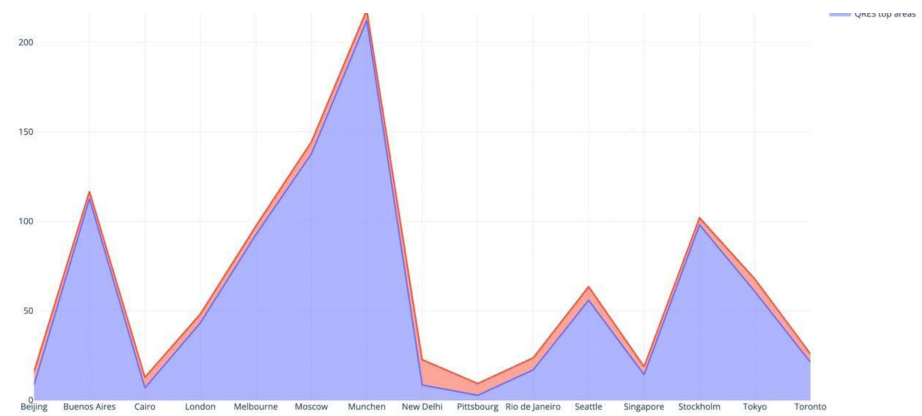

Figure 10:
Most livable areas, QRES vs GH

By comparing all the methods (Figure 12), we can observe different trends. Considering the different approaches and sources, this graph may offer researchers the opportunity to delve deeper into these cities to determine whether the observed performance variations are systemic or influenced by the different methods.

One of the most interesting applications of the .csv output is the ability to analyze the performances of different areas within a city.

In Figure 13, we examined how each point in the Palermo district performs, alongside its total resilience (depicted in green). It is evident that the “R_Shops” feature scores remarkably high. Moreover, there are areas with notably low scores located near or above the sea, while the central areas of Palermo exhibit a more consistent performance trend.

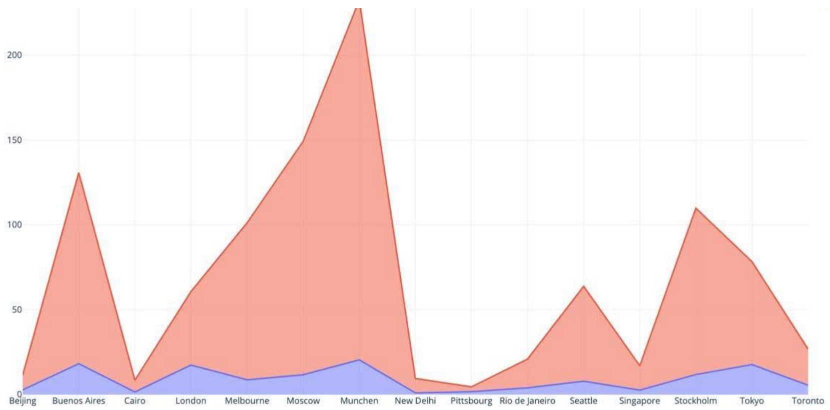

Figure 11:
QRES: cities R average, vs most liveable areas

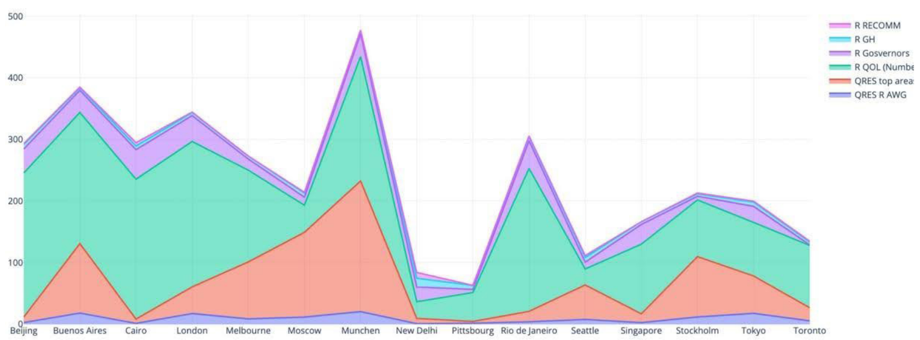

Figure 12:
QRES: cities R average, vs most liveable areas

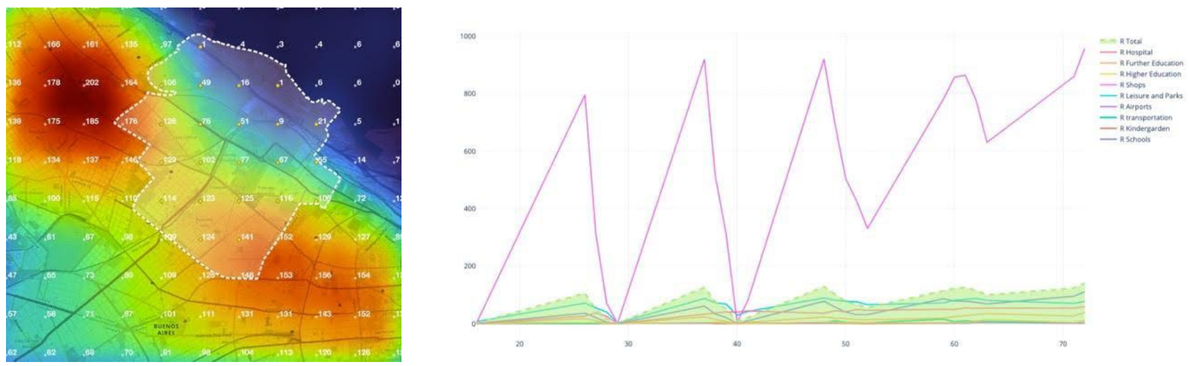

Figure 13:
Performance of the Palermo district

4. RESULTS

The QRES plugin is presented here in its first iteration. We foresee being able to publish it to the QGIS repository with the next version. This study enabled us to assess the tool’s potentials. The plugin generates an effective visualization, with the resilience values clearly distinguishable through a heat map. Moreover, users have the flexibility to customize the color scheme and parameters of the heat map for specific research purposes and to ensure accessibility for individuals with special needs. The attribute table generated by the plugin can be exported as a .csv file for further data analysis and visualization outside of QGIS.

5. CONCLUSIONS

The QRES plugin demonstrates significant potential and offers a valuable tool for urban planners and designers to swiftly assess the resilience potential of cities at various scales and with the appropriate resolution. The workflow is user-friendly, seamlessly integrated within QGIS, one of the most widely used GIS software platforms, particularly for the implementation of functions tailored by researchers. The graphic output enhances accessibility for the general public, as they are more likely to engage with graphics over raw data. The tests conducted for this paper not only validated our previous findings but also provided a means to gauge the quality of the results. The next phase of our research involves gathering feedback from a more diverse and expansive user base to address interface and performance considerations.

While the plugin functions effectively and delivers the required results, performance is a critical aspect that demands attention, and we are committed to further exploring methods to expedite this process. Further iterations will include ways to optimize the computations (with both cloud-based and local solutions).

In the future, we intend to provide users with greater options to fine-tune their analyses: select specific features, explore alternative formulas for calculating R, and introduce the possibility of adding new features to predict how the city’s performance would be impacted by their introduction.

REFERENCES

ARUP and Rockefeller Foundation. (2014) *City Resilience Framework*. London, UK: ARUP.

Bottazzini, U., Blåsjö, V. (2017) Chapter 4 - Mathematical context. In Bottazzini, Umberto, Blåsjö, Viktor (eds). *Studies in the History of Mathematical Inquiry*. Transcendental Curves in the Leibnizian Calculus. Academic Press, pp. 61-100. https://doi.org/10.1016/B978-0-12-813237-1.50004-1.

Bungalow. (2023) *The 9 best neighborhoods to live in Seattle, Bungalow*. Available at: https://bungalow.com/articles/best-neighborhoods-in-seattle-wa (Accessed: 26 October 2023).

Carta, S., Pintacuda, L., Owen, I.W. and Turchi, T. (2021) Resilient communities: a novel workflow. *Frontiers in Built Environment* 7, p. 767779.

Carta, S., Turchi, T. and Pintacuda, L. (2022) Measuring Resilient Communities: An analytical and predictive tool. CAADRIA 2022 Proceedings.

Carta, S., Turchi, T., Pintacuda, L. and Jankovic, L. (2023). RECOMM. Measuring resilient communities: An analytical and predictive tool. *International Journal of Architectural Computing* 21(3): 536-560.

Carta, S., Turchi, T., Spencer, N. and Calvet, M.V. (2022). Encoding Social Values of Local Communities in Algorithmic-Driven Design Methods. In *International Symposium on Formal Methods in Architecture* (pp. 435-452). Singapore: Springer Nature Singapore.

Cooper, C.H.V., Chiaradia, A.J.F. (2020) sDNA: 3D-d spatial network analysis for GIS, CAD, Command Line & Python. *SoftwareX* 12: 100525. https://doi.org/10.1016/j.softx.2020.100525

Department for Transport. (2014) *National Travel Survey Travel to School*. Online Report available at: https://assets.publishing.service.gov.uk/government/uploads/system/uploads/attachment_data/file/476635/travel-to-school.pdf

Dianat, H., Wilkinson, S., Williams, P. and Khatibi, H. (2022) Choosing a holistic urban resilience assessment tool. *International Journal of Disaster Risk Reduction* 71, p. 102789.

Dogan, T., Yang, Y., Samaranayake, S. and Saraf, N. (2020) Urbano: A tool to promote active mobility modeling and amenity analysis in urban design. *Technology | Architecture+ Design* 4(1), pp. 92-105.

Gadzinski, J. (2015) *The Impact of Local Transport Systems on Green Infrastructure – Policy Versus Reality: The Case of Poznan*, Poland. Urbani Izziv, 26, S65–S83.

Government Office for Science. (2019) *A time of unprecedented change in the transport system*. Online Report available at: https://assets.publishing.service.gov.uk/government/uploads/system/uploads/attachment_data/file/780868/future_of_mobility_final.pdf

Grosvenor. (2014) *Resilient Cities: A Grosvenor research report*. Available at: https://www.preventionweb.net/publication/resilient-cities-grosvenor-research-report

Jha, A.K., Miner, T.W. and Stanton-Geddes, Z. eds. (2013). *Building urban resilience: Principles, tools, and practice*. World Bank Publications.

Khazai, B., Anhorn, J. and Burton, C.G. (2018) Resilience Performance Scorecard: Measuring urban disaster resilience at multiple levels of geography with case study application to Lalitpur, Nepal. *International journal of disaster risk reduction* 31, pp. 604-616.

Knupfer, SM. (2018) *Elements of Success: Urban Transportation Systems of 24 Global Cities*. London: McKinsey and Co. Online Report available at: https://www.mckinsey.com/~/media/McKinsey/Business_Functions/Sustainability/Our_Insights/Elements_of_success_Urban_transportation_systems_of_24_global_cities/Urban-transportation-systems_e-versions.ashx (2018).

Kolmar, C. (2022) *Best Seattle suburbs to live in for 2022*. HomeSnacks. Available at: https://www.homesnacks.com/best-seattle-suburbs/ (Accessed: 26 October 2023).

Kronberg, N. (2019) *Transport statistics Great Britain 2019*. Department for Transport, Online Report available at: https://assets.publishing.service.gov.uk/government/uploads/system/uploads/attachment_data/file/870647/tsgb-2019.pdf

Nakaya, T., & Yano, K. (2010) Visualising Crime Clusters in a Space-time Cube: An Exploratory Data-analysis Approach Using Space-time Kernel Density Estimation and Scan Statistics. *Transactions in GIS* 14(3): 223-239. ISSN 1361-1682. doi: 10.1111/j.1467-9671.2010.01194.x.

Numbeo. (2021) Quality of Life Index by City 2021. Available at: https://www.numbeo.com/quality-of-life/rankings.jsp

O'Sullivan, D., Morrison, A. and Shearer, J. (2000) Using desktop GIS for the investigation of accessibility by public transport: Aan isochrone approach. *International Journal of Geographical Information Science* 14(1), pp. 85-104.

SAVA. (2022) *The best neighborhoods of Buenos Aires, from Palermo to Puerto Madero, South American Vacations*. Available at: https://www.savacations.com/best-neighborhoods-buenos-aires-palermo-puerto-madero/ (Accessed: 26 October 2023).

Sharifi, A. and Yamagata, Y. (2016) Urban resilience assessment: Multiple dimensions, criteria, and indicators. *Urban resilience: A transformative approach*, pp. 259-276.

Tapsuwan S, Mathot C, Walker I, et al. (2018) Preferences for sustainable, liveable and resilient neighbourhoods and homes: A case of Canberra, Australia. *Sustainable Cities and Society* 37: 133–145.

Thompson, A. W., Prokopy, L. S., Floress, K., & Weinkauf, D. C. (2011). A Method for Incorporating Community Priorities into GIS: Challenges, Choices, and Directions for Landscape Planners. *Landscape Journal* 30(2): 299–312. http://www.jstor.org/stable/43324380

Wardekker, A., Wilk, B., Brown, V., Uittenbroek, C., Mees, H., Driessen, P., Wassen, M., Molenaar, A., Walda, J. and Runhaar, H. (2020) A diagnostic tool for supporting policymaking on urban resilience. *Cities 101*, p. 102691.